Received: 4 December 2020 | Revised: 25 May 2021 | Accepted: 25 May 2021

DOI: 10.1002/app.51296

ARTICLE

Journal of Applied Polymer Science WILEY

Synthesis and characterization of the properties of thermosensitive elastomers with thermoplastic and magnetic particles for application in soft robotics

Nina Prem[1] | **Florian Schale**[1] | **Klaus Zimmermann**[1] | **Darshan Kare Gowda**[2] | **Stefan Odenbach**[2]

[1]Technische Universität Ilmenau, Ilmenau, Germany

[2]Technische Universität Dresden, Dresden, Germany

Correspondence
Nina Prem, Technische Universität Ilmenau, Ilmenau, Germany.
Email: nina.prem@tu-ilmenau.de

Funding information
Deutsche Forschungsgemeinschaft, Grant/Award Numbers: ZIM 540/20-1, OD 18/28-1

Abstract

In the currently rapidly developing field of soft robots, smart materials with controllable properties play the central role. Thermosensitive elastomers are soft, smart materials whose material properties can be controlled by changing their temperature. The aim of this work is to investigate the mechanical properties, to analyze the surface, the inner structure, and the heat transfer within the thermosensitive elastomer materials. This should provide a knowledge base for new combinations, such as a combination of thermosensitive and the well-known magneto sensitive elastomers, in order to realize new applications. Thermoplastic polycaprolactone particles were incorporated into a flexible polydimethylsiloxane matrix to produce thermosensitive elastomer samples. With a low melting point in the range of 58–60°C, polycaprolactone offers good application potential compared to other thermoplastic materials such as polymethamethylacrylate with a melting point above 160°C. Test samples of different material compositions and geometries were made to examine temperature-depending material properties. Two useful effects were identified: temperature-dependent change in stiffness and the shape memory effect. In certain examinations, carbonyl iron particles were also included to find out if the two particle systems are compatible with each other and can be combined in the polydimethylsiloxane matrix without disadvantages. Changes in shore hardness before and after the influence of temperature were investigated. Micro computed tomography images and scanning electron microscopy images of the respective samples were also obtained in order to detect the temperature influence on the material internally as well as on the surface of the thermosensitive elastomers in combination with carbonyl iron particles. In order to investigate the heat transfer within the samples, heating tests were carried out and the influence of different particle concentrations of the thermosensitive elastomers with and without carbonyl iron particles was

determined. Further work will focus on comprehensive investigations of thermo-magneto-sensitive elastomers, as this will enable the functional integration in the material to be implemented with increased efficiency. By means of the different investigations, the authors see future applications for this class of materials in adaptive sensor and gripper elements in soft robotics.

KEYWORDS
elastomers, mechanical properties, spectroscopy, thermal properties, thermoplastics

1 | INTRODUCTION

The increasing tendency to integrate extensive functions in a single smart material instead of separated components with distinct material properties, processing of energy and information, leads to their steadily growing importance. For example, magnetic hybrid materials such as magneto sensitive elastomers (MSEs) offer the potential to possess such complex properties.[1] MSEs ordinarily consist of non-magnetic elastic polymer matrices, in which soft or hard magnetic particles are embedded. The size of these particles is generally limited to the nm to μm range. This type of smart material shows multi-functional field-dependent properties under the influence of an external magnetic field. Examples are the elastic and plastic properties of MSEs, which may be isotropic or anisotropic and are magnetically controllable. These controllable material properties are induced by the interaction of both components (magnetic filler and elastomer), thereby the compound is exceeding the usability of each solitary component.[2] Beyond that these properties can be set during MSE's production by prior application of magnetic fields, mechanical stresses and preliminary treatment of the filler particles.[3–5] Smart materials can also consist of an elastic matrix and electrically conductive fillers, which causes the actual insulator to become electrically conductive, resulting in the so-called electroactive polymers (EAPs).[6] Due to these controllable physical material properties, there is a great interest especially in the fields of (soft) robotics, medical engineering, and so forth.[7] The various fabrication methods are also increasingly being researched. For example, not only thermoplastics but also MSEs and EAPs can now be formed into a specific shape using 3D printing technology. This enables materials to be produced more quickly and flexibly in different designs and to be tuned individually according to specific requirements.[8] After numerous studies in this extensive field of smart materials mentioned above, the focus changed to materials that can be thermally influenced. The additional thermal influence on different polymers, which are not considered smart materials by themselves, was already investigated especially in the medical field.[9–11] This work is focused on a practical aspect of thermoelastic effects within a polymer compound and not only in a single polymer type. The developed thermosensitive elastomers (TSE) made of the combination of an elastic polydimethylsiloxane (PDMS) matrix with thermoplastic particles enables to change their material properties through the influence of temperature change. The advantage is that the materials have to be heated up to a maximum of 70°C, because of the low melting point of the thermoplastic polycaprolactone (PCL) filler particles. In the presented work, the main focus lies on systematic investigations, consisting of mechanical analysis such as the measurement of stress–strain curves through tensile and compression tests of TSE itself. Thereby it is one of the key parameters in controlling their change of stiffness. Additionally, the shape memory effect (SME) is examined. Furthermore, measurements of shore hardness, as well as thermal and structural analysis of TSE with carbonyl iron particles (CIP) were carried out. In this class of hybrid materials, the distribution of particles play also an important role in determining their macroscopic properties. The resulting hybrid material enables new applications with a controllable material characteristic for the use in soft robotic systems, especially on the generation of adaptive mechanical compliance of technical functional elements, such as actuators and sensors. Above all, the different change in stiffness due to the PCL particles or CIP makes a combination of MSE and TSE interesting, as this could expand the application possibilities. However, in order to achieve these results, the TSEs and the compatibility with CIP need to be examined and properly understood first.

2 | EXPERIMENTS

2.1 | Materials and samples fabrication

The thermosensitive elastomer used in this work consists of an addition-curing RTV-2 silicone, a PDMS, as matrix and thermoplastic PCL particles (PCL MW 50,000 from Polysciences). Thereby the RTV-2 silicone can be produced

with a different shore hardness (Shore 0–17). Curing is achieved by mixing the two PDMS components in a specific mass ratio. A different ratio of the base or the catalyst generally leads to an incomplete curing. The vulcanization commences on physical contact between crosslinker and catalyst, takes place at temperatures above 10°C, and is accelerated using higher temperatures up to 200°C if necessary. In contrast to other silicone types the vulcanization speed is controlled exclusively by temperature.[12] Since there is no generation of secondary products and no possibility of weight loss during vulcanization, the material is not subjected to shrinkage.[13] Initially the PDMS components were admixed before being combined with the PCL particles, which have a melting point in the range of 58–60°C and a particle size below 600 µm. CIP type SQ (BASF) with an average particle size of 3.9–5 µm and a spherical shape were also added to the composite material described above. These particles were preferred to other hard or soft magnetic particles on account of their uncomplicated handling. In addition, there is a wide range of experience in the production as well as numerous investigations on the influence of the particles in combination with the so-called MSE.[3,6] In this case, the remaining question is whether a combination of the two particle groups (soft magnetic and thermoplastic particles) in an elastic matrix is appropriate. The different mixtures are specified in detail in the respective chapters. Samples were produced by mixing of the proportioned material components in a mixer at room temperature (25°C). For this use, an acceleration of the crosslinking process is not required and due to the melting point of the included PCL particles, the crosslinking process should not take place at temperatures above 58°C.

Degassing of the samples under adequate process vacuum followed. The addition curing RTV-2 silicone has a low mixing viscosity, which facilitates mixing with other material components. Its permanent temperature resistance up to 200°C, and the fact that the RTV-2 silicone is still capable of repeated deformation without damage within the described experiments at the appropriate load, provides a material basis for testing possible shape memory properties.[14,15] In addition, due to the high temperature resistance of the PDMS, a thermal insulation layer encloses the embedded PCL particles. Figure 1 depicts the different sample geometries for the subsequent investigations.

Seven different sample sets per PDMS Matrix were prepared, see Table 1. These mixtures were prepared for each analytical method and the corresponding geometries, except when it is explicitly mentioned in the respective section that other sample mixtures were used. The most important combinations are: PDMS as the matrix itself; PDMS with 5 wt% PCL and PDMS with 20 wt% PCL as two extreme values of the thermoplastic percentage, (minimum and maximum amount of PCL particles); PDMS with 5 wt% PCL and 15 wt% CIP and PDMS with 15 wt% PCL and 5 wt% CIP as a maximum mixture of the PDMS matrix, PCL particles and CIP.

The density of the tensile and compression samples was determined prior to the respective measurements and representative for the other sample geometries. It is obvious that the sample density increases with higher PCL particle concentration and CIP concentration. PDMS is a wide-meshed elastomer with a metered density of 1.078–1.081 g/cm^3 (Silikonfabrik), adding PCL with an average density of 1.145 g/cm^3 (Polysciences) and CIP with an average density of 7.8 g/cm^3 (BASF)

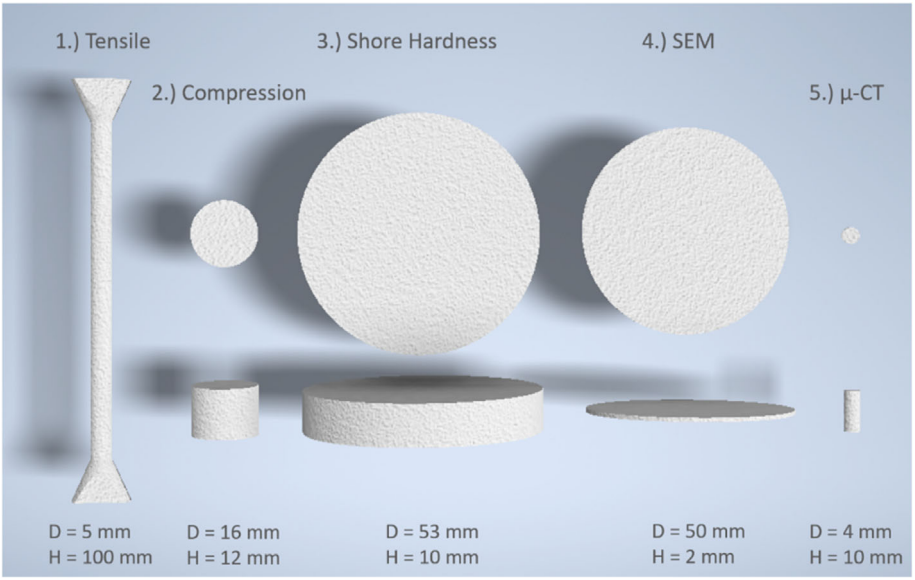

FIGURE 1 Different sample geometries for (1) tensile, (2) compression, (3) shore hardness, (4) scanning electron microscope (SEM), (5) micro computed tomography (µ-CT) [Color figure can be viewed at wileyonlinelibrary.com]

causes a mixed density. This can be calculated from the respective density values and the relevant percentages in the composite material shown in the following equation.

$$\mathrm{wt\%} \cdot \rho(\mathrm{PDMS}) + \mathrm{wt\%} \cdot \rho(\mathrm{PCL}) + \mathrm{wt\%} \cdot \rho(\mathrm{CIP}) = \rho(\mathrm{Mixture}).$$

The theoretically calculated values are compared with the average density of the samples in Table 2, whereby a significant increase can be recognized. The reason is that the PCL particles and CIP occupy the spaces within the wide-meshed network until they are able to form a secondary network themselves by an increasing percentage within the compound.[16,17] Additionally, deviations and fluctuations from the theoretically calculated values could be due to the measuring method itself.

2.2 | Heat transfer

This examination serves not only for heat transfer analysis per se but also as a preliminary examination for all following testing methods in order to better estimate the duration of the necessary temperature exposure. All sample geometries illustrated in Figure 1, except scanning electron microscopy (SEM) samples were prepared as described in the previous chapter with the known compositions. After the non-crosslinked sample mixtures were poured into the specific molds, a PT100 temperature sensor was placed in the center of the samples. Therefore, the sensor represents a centered particle of the size 1 x 1 mm^2 and indicates when the core of the sample has reached a certain temperature. The prepared samples were heated to 27°C to ensure that each embedded sensor would measure the same starting temperature.

The different samples were then placed in a laboratory furnace at 60°C and the respective values of the PT100 sensor were recorded. In Figure 2, the different sample geometries and mixtures, dependent on the time taken for the center of each sample to reach 60°C, are compared. The results shown in Figure 2 clearly demonstrate that the heat transfer of both geometries, the micro computed tomography (μ-CT) and tensile samples, reached the temperature inside the respective samples after a very short time, on the contrary to the geometry of the shore hardness samples. The reason for these differences is due to the geometry itself. The sample diameter at the sensor position of the μ-CT and tensile samples is smaller than the sample diameter at the sensor position of the shore hardness samples. In addition, each sample and sample geometry clearly indicates that the heat transfer of sample E (20) is the slowest, whereas sample F (5, 15) as well as sample A (0) is the fastest to reach 60°C in the center, see Figure 3. Polymers such as PDMS commonly have small thermal conductivities (0.18 W/mK under ambient conditions[18]), which can be improved or deteriorated by adding specific fillers.[19] Heat transfer within an elastomer such as PDMS works similarly to many other solids through the elastic bonding forces between the particles.

If a particle is set into oscillation due to a raise in temperature at a certain point, the elastic bond coupling will also cause the neighboring particles to oscillate. Energy

TABLE 1 Different samples and their abbreviation

Sample mixtures	Abbreviation
PDMS	A (0)
PDMS with 5 wt% PCL	B (5)
PDMS with 10 wt% PCL	C (10)
PDMS with 15 wt% PCL	D (15)
PDMS with 20 wt% PCL	E (20)
PDMS with 5 wt% PCL and 15 wt% CIP	F (5, 15)
PDMS with 15 wt% PCL and 5 wt% CIP	G (15, 5)

Abbreviations: CIP, carbonyl iron particles; PCL, polycaprolactone; PDMS, polydimethylsiloxane.

TABLE 2 Average density of tensile and compression samples compared with the theoretical calculated density

	Density (g/cm^3)		
Sample mixtures (abbreviations)	Tensile samples	Compression samples	Theoretical values
Sample A (0)	1.078	1.080	1.078–1.081
Sample B (5)	1.097	1.101	1.082
Sample C (10)	1.121	1.125	1.085
Sample D (15)	1.138	1.139	1.089
Sample E (20)	1.146	1.151	1.092
Sample F (5, 15)	2.120	2.125	2.090
Sample G (15, 5)	1.462	1.469	1.425

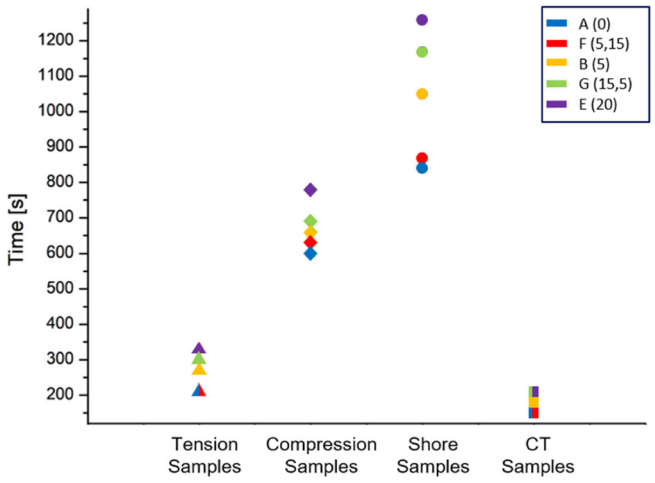

FIGURE 2 Time needed to achieve 60°C in the center of each geometry with different compositions [Color figure can be viewed at wileyonlinelibrary.com]

can thus be transferred from particle to particle. The thermal conductivity of PDMS is reduced by the addition of PCL particles. PCL has a thermal conductivity of 0.26 W/mK under ambient conditions[20] and melt between 58 and 60°C. If a mixture with PCL particles is heated instead of an homogeneous matrix like the PDMS itself, the PCL particles first absorb energy during the melting process. Once the melting process of the PCL particles at the edges of the sample is completed, thermal energy can be transported further into the center of the sample. However, if the mixture also contains CIP with high thermal conductivity (79.5 W/mK), the process of thermal energy transfer is decelerated at one point (PCL particles) and accelerated at another point (CIP).If the mixture consists of a higher percentage of CIP, the samples heat up to the center faster as bulk PDMS.[21,22] This effect can even be increased if an external magnetic field is applied during the manufacturing of the composition causing the

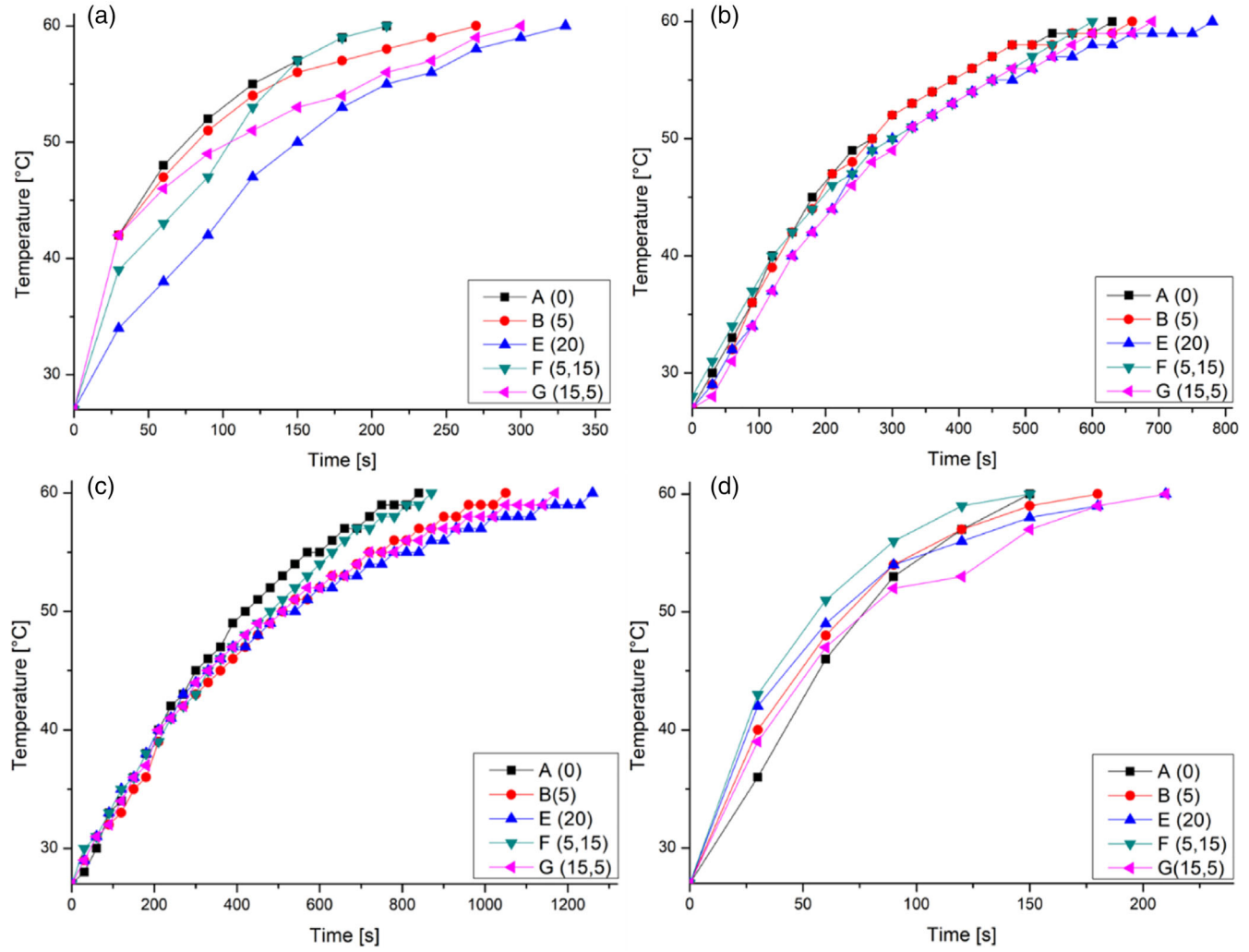

FIGURE 3 Heat transfer depending on time of (a) tension, (b) compression (c) shore hardness and (d) μ-CT samples [Color figure can be viewed at wileyonlinelibrary.com]

particles to form chain-like structures within the matrix. This leads to effective thermal paths within the composite material.[23] If the CIP mass is lower than the PCL mass (sample G (15, 5)), the sample heats up very slowly, but faster than sample E (20).

2.3 | Compression and tension tests

A metal heating chamber was developed especially for tension and compression experiments. The method of heating the sample by means of a metal heating chamber with proper thermal sealing utilizes the thermal conductivity achieved directly by contact heat conduction (metal adapter) and indirectly by thermal convection (air in the chamber). For this purpose, thermally stationary simulations were performed to ensure the optimal design of the heating chamber. Figure 4(a) illustrates the ideal chamber, which represents a closed system. To more accurately reflect reality and to integrate the adapter to the compression and tensile testing machine, further analysis were carried out, see Figure 4(b),(c).

The final measurement setup for compression and tensile tests is illustrated in Figure 5(a),(b). The advantage of

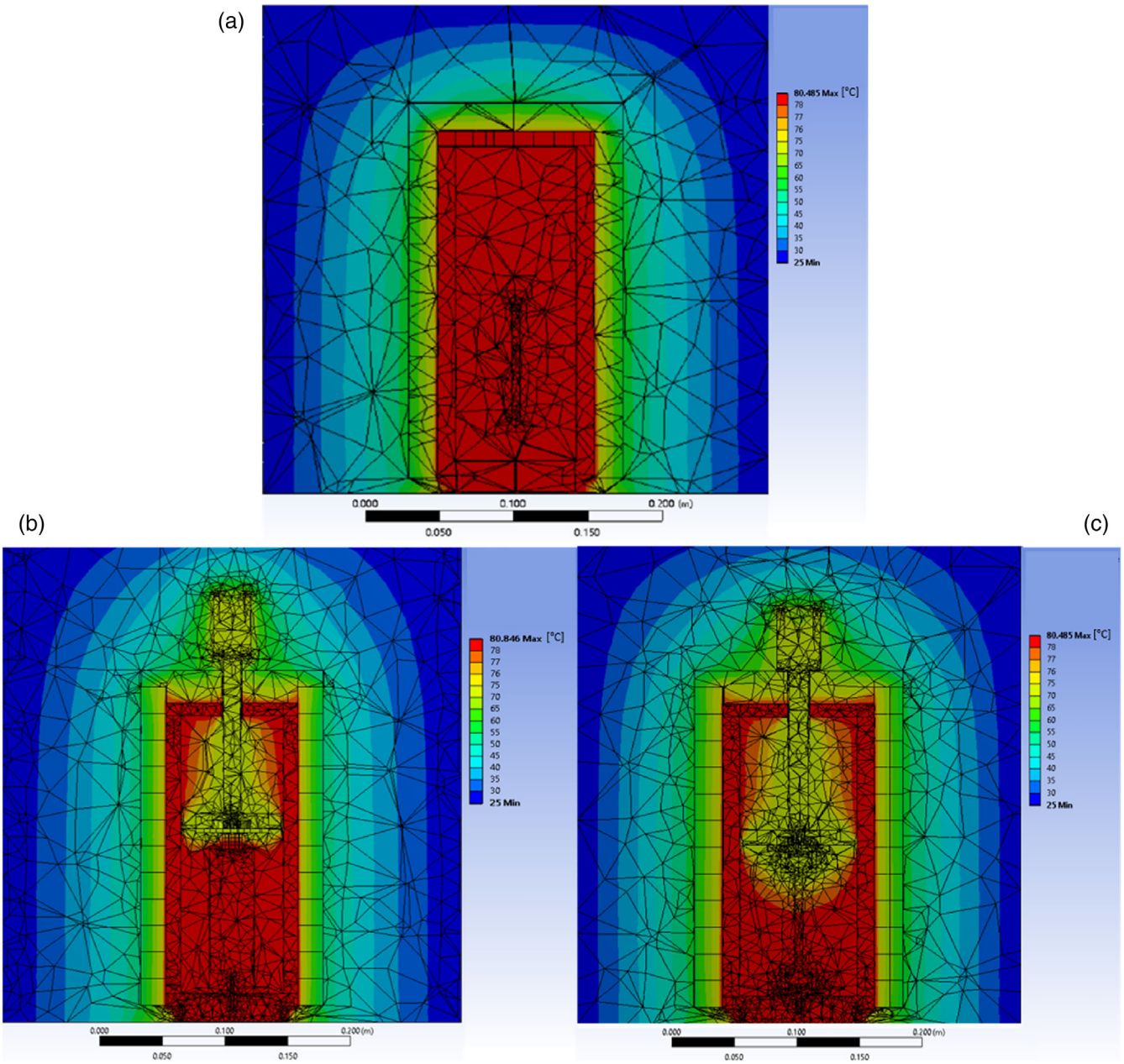

FIGURE 4 Heating chamber for compression and tension tests (a) ideal case. Heating chamber with an aluminum adapter for (b) compression and (c) tension tests [Color figure can be viewed at wileyonlinelibrary.com]

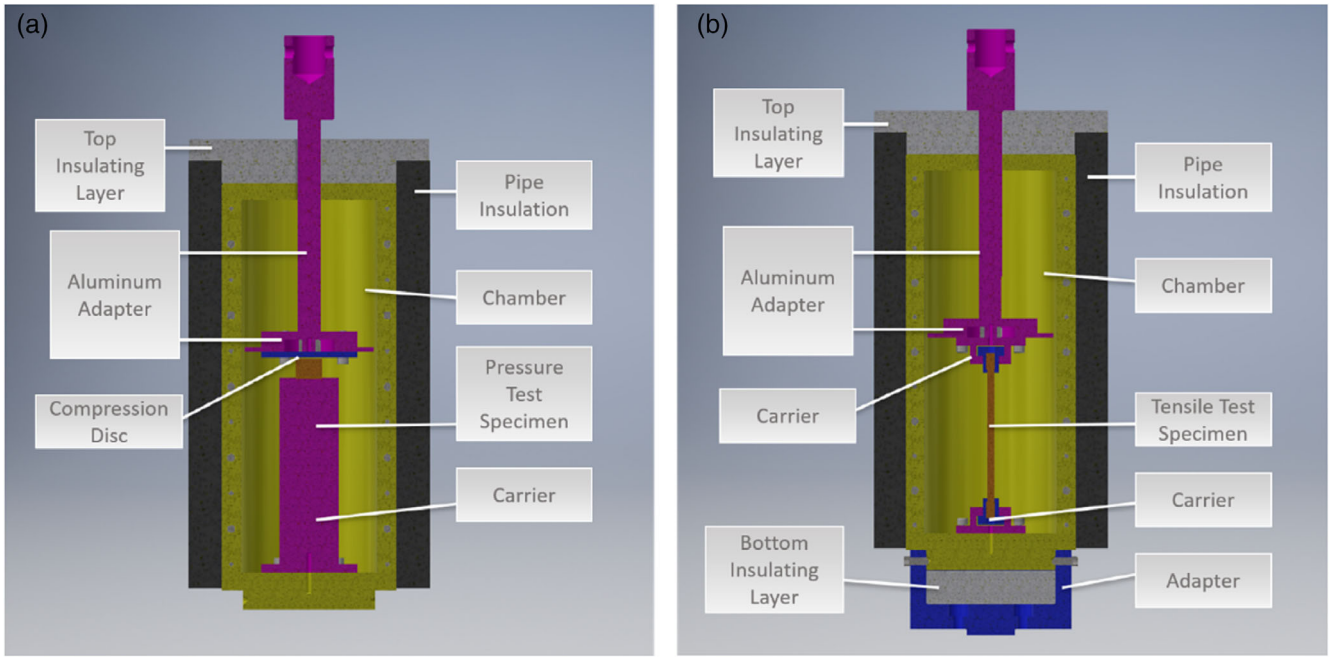

FIGURE 5 Heating chamber for (a) compression and (b) tension tests [Color figure can be viewed at wileyonlinelibrary.com]

this heating method is that the inside of the closed and insulated heating chamber leads to a stationary temperature distribution after long-term heating, which results in a very even temperature gradient of the sample. Although thermal conduction is essentially responsible for heating the sample, the influence of thermal convection and thermal radiation on the heat distribution within the heating chamber cannot be neglected. The tensile and compression testing machine, a Zwick test machine Z005 by ZwickRoell GmbH and Co, is subsequently connected to this heating chamber by means of an adapter.

The measurement setup for compression tests is illustrated in Figure 5(a). The compression samples are cylindrical with a height of 12 mm and a diameter of 16 mm, see Figure 1. First, the compression test is pre-treated according to the Mullins Effect and the corresponding compression test standards for elastomers. This pre-treatment process is also called preconditioning. The preconditioning of the compression test sample passes through the entire test phase in order to unify and standardize the test steps. Secondly, the compression samples are examined in the temperature range of 55–70°C to determine the specific temperature of the thermosensitive effect of the composite elastomer. The TSE material was checked for a possible SME afterwards. Considering that the compression test is based on elastomeric material, its mechanical response corresponds to the Mullins effect, that is, its stress–strain curve depends on its initial maximum load. If the same load test is performed several times on the elastomer sample, the stress–strain behavior of the elastomer sample will be softer in the subsequent load cycles than in the first load cycle.[24,25] This is due to the fact that under the load, the inner structure of the elastomer is partially broken during deformation and proportionally re-formed. This means that the macromolecular chain of the elastomer deteriorates due to the Mullins Effect, which results in a change of the elastomers structure and the embedded particles of the elastomer are separated from each other.[26,27] The advantage of the preconditioning process is the ability to improve the stability of the inner structure of the elastomer sample and to ensure standardized initial conditions for all elastomer samples utilized in the investigation. Since the effects are the highest with a mixture of PDMS and 20 wt% PCL (sample E (20)), exclusively the results of these experiments are presented in the following. Consequently, these sample mixture is preferred for further mechanical investigations and applications. Moreover, no CIP were added in this case. It is known from previous investigations that the CIP in an elastomer as a MSE lead to an increase in stiffness under the influence of an external magnetic field.[28,29] Since the TSE material should soften when the temperature is increased, it serves no purpose to increase the stiffness of the material by applying an external magnetic field during the softening of the TSE. The important aspect is whether the assumption that the stiffness decreases with temperature is correct. In later applications, the controversial function of the two particle groups within the material could be used beneficially. In order to determine the temperature sensitivity of the composite elastomer as already

mentioned above, the samples were subjected to a compression test at various temperatures (55–70°C). After each heating period of 6000 s and testing, the compression sample is cooled down to room temperature. Figure 6(a) shows the relation between compression stress and compressed distance. It is apparent that there is almost no change in the curve at 55–58°C, while the force stays at a high level, which could indicate that the PCL particles embedded in the elastomer have not melted or only a very small proportion has melted. The curve at 60°C represents a temperature threshold has been reached, as low temperatures have only little effect on the measurement results and higher temperatures develop towards a force limit. It can therefore be assumed that between 58 and 60°C the PCL particles in the composite elastomer will begin to melt. Although after 58°C the force starts to decrease with increasing temperature, there is a slight difference between the curves in the range of 65–70°C, which indicates that 65°C is already a limit for thermal sensitivity effects. It can be concluded that the stress change of the elastomer is mainly influenced by the temperature. Therefore, the compound material can be considered a TSE.

The measurement setup for tensile tests is illustrated in Figure 5(b). The sample geometry is shown in Figure 1. The relevant diameter is 5 mm, while the height of the middle part is 100 mm. The samples for the tensile measurements were also preconditioned, because of the Mullins effect. After preconditioning the samples were subjected to a tension test at various temperatures (55–70°C). The results are illustrated in Figure 6(b) using sample E (20) for the afore-mentioned reasons. It can be observed that 60°C also forms a temperature threshold in this case. At 55–58°C, the required stress is higher than at 60°C at the same elongation. The reason for this is that the PCL particles start to melt at 58°C, after all particles have melted the resistance to tensile stress is now lower than at lower temperatures when the particles are in their original plastic form as already proven by the compression measurements. The same as for the compression test also applies here for the temperatures above the temperature threshold of 60°C. The resistance to tensile stress is lower up to 65°C as the limit for thermal sensitivity effects. In order to confirm a possible SME of the TSE, the following verification experiments are performed:

1. The height of a compression sample E (20), in its initial state (at room temperature after preconditioning) is measured and recorded (t0, Figure 7).
2. The sample is heated from room temperature to 70°C and then compressed by 4 mm from the original height of 12 mm, maintaining this height (8 mm) and the applied load for 20 min until the sample has naturally cooled down to room temperature (t0H, Figure 7).
3. After sufficient cooling of 12 h, the load on the sample is removed and the height of the sample is measured and recorded again (t1, Figure 7). At the same time, the height of the sample is measured after a series of time intervals (t2–t9, Figure 7).
4. The sample is heated from room temperature to 70°C and the height of the sample is measured again after it is cooled down to room temperature (t10H, Figure 7).

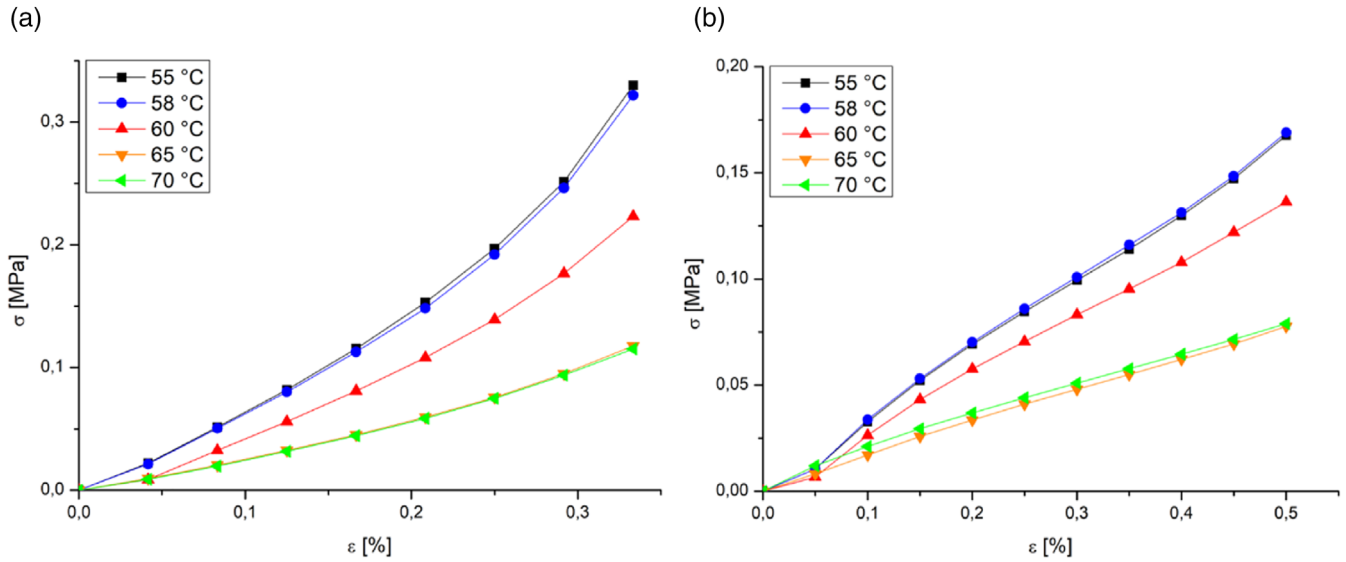

FIGURE 6 Sample E (20) (a) compression and (b) tension tests depending on different temperatures [Color figure can be viewed at wileyonlinelibrary.com]

The progression of the following heights are illustrated in Figure 7. It can be concluded that the sample has maintained a certain deformation state over a long period after cooling and at the same time can quickly restore the original shape after heating and the corresponding heating time (see Section 2.2, heat transfer). This means the time taken to deform the sample during heating corresponds to the time taken for the sample to regain its original shape. The height after regeneration is lower than the initial height. It is assumed, in this case, that this is caused by the reconstitution of the internal structure of the sample and the positional error during the height measurement. In principle, it can be assumed that the elastomer with PCL particles has a usable SME and can be called shape memory polymer (SMP).[30,31]

In Figure 8, an image of the sample E (20) and G (15, 5) in their initial state was made (1). Subsequently, these samples were bent at 70°C for 15 min and cooled down to room temperature, but still be bent. After removing the force, the samples retain the bent state (2), until they are heated up again to 70°C (3).

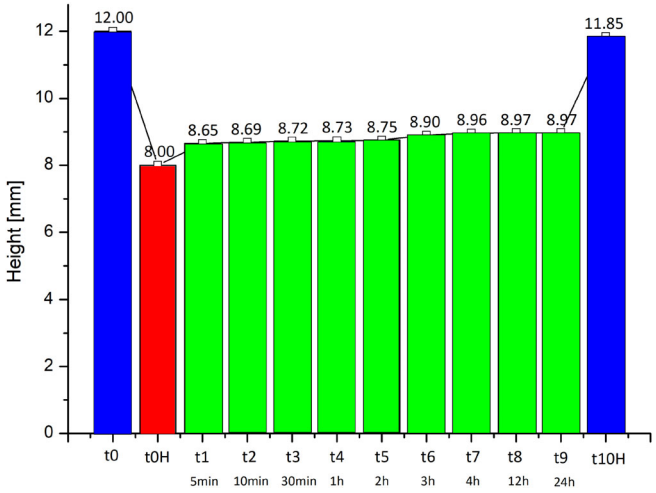

FIGURE 7 Shape memory effect of sample E (20) [Color figure can be viewed at wileyonlinelibrary.com]

2.4 | Shore hardness

With the described examination methods, mechanical material characteristics can be determined, but this also includes the investigation of the hardness of a material. Hardness is the resistance that a material offers to an indenting body. Higher measured values imply greater resistance to indentation and hence harder materials. A test sample is pressed into the material to be investigated and a partly plastic, partly elastic-returning impression is created.[32] Shore hardness 0 and A (DIN ISO 7619-1 and DIN 53505/00) are a quick and convenient way to measure hardness for soft polymers and elastomers. Thereby the thickness of the respective samples plays an important role. According to[33] the samples should have a minimum thickness of 6 mm. The measured values obtained with a Shore 0 hardness tester on samples less than the specified thickness of 6 mm result in erroneously high values, with the error increasing as the thickness decreases. The samples utilized and measured are illustrated in Figure 1. The shore hardness tester or durometer (Sauter HB0 100–0 mit Prüfstand TI-A0) in this work measures the depth of an indentation in the material created by a given force on a standardized indenter. The samples were first measured at room temperature, then heated at 60°C for the time corresponding to the results of the thermal behavior analysis. Afterwards the samples were cooled down to room temperature and measured once again. The results are shown in Table 3. There are two effects to be recognized. The first effect is the increasing hardness value the more PCL particles are contained

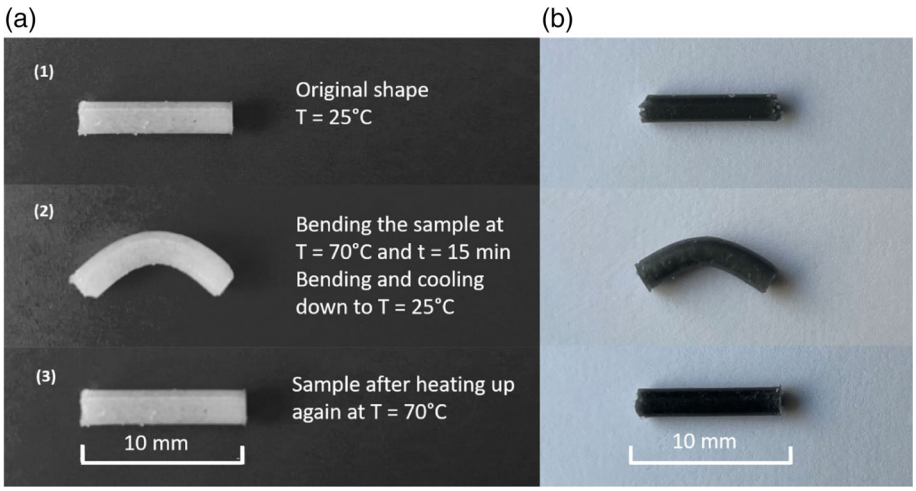

FIGURE 8 Shape memory effect of (a) E (20) and (b) G (15, 5) [Color figure can be viewed at wileyonlinelibrary.com]

in the compound. The CIP also increase the hardness value, but not as much as the PCL particles. One reason for this may be the size and shape of the respective particles. While the PCL particles are <600 μm in size and have no particular shape, the CIP are <5 μm in size and spherical. The second effect is that the hardness values at room temperature and after the temperature treatment of 60°C are virtually the same (measuring error of the measuring device is ±1 Shore). The particles consequently increase the hardness of the composite material. The unchanged hardness values before and after temperature treatment are due to the fact that the PCL particles return to their original form with the original properties after they have been melted and cooled down again to room temperature, while the CIP remain unchanged embedded in the silicone during this process.

TABLE 3 Shore hardness of different samples before and after temperature treatment

Sample mixtures (abbreviations)	Shore hardness (shore 0)	
	Prior melting (original state, at 24°C)	After melting (and cooling down to 24°C again)
A (0)	5.8	4.6
B (5)	7.4	7.8
C (10)	9.8	10
D (15)	12.8	12.6
E (20)	15.8	15.4
F (5, 15)	10.8	10.4
G (15, 5)	14.0	13.8

2.5 | Scanning electron microscope

The examination with the SEM (Hitachi S - 4800 with energy-dispersive X-ray [EDX]-system) serves the micro morphological investigation of the surfaces of different samples. The focus is thereby:

1. The general surface visualization of the respective samples,
2. The size measurement of the respective filler particles to be able to confirm the shape and size of the particles,
3. EDX-images of the samples to differentiate the particles from each other and to differentiate the particles from the matrix.

The investigations confirmed the assumption that due to the limited measurement area no difference between 20 wt% PCL particles and 15 wt% PCL particles could be detected, as well as no difference between 10 wt% PCL particles and 5 wt% PCL particles. The same is valid for the respective CIP mass percentage, PDMS with 10 wt%

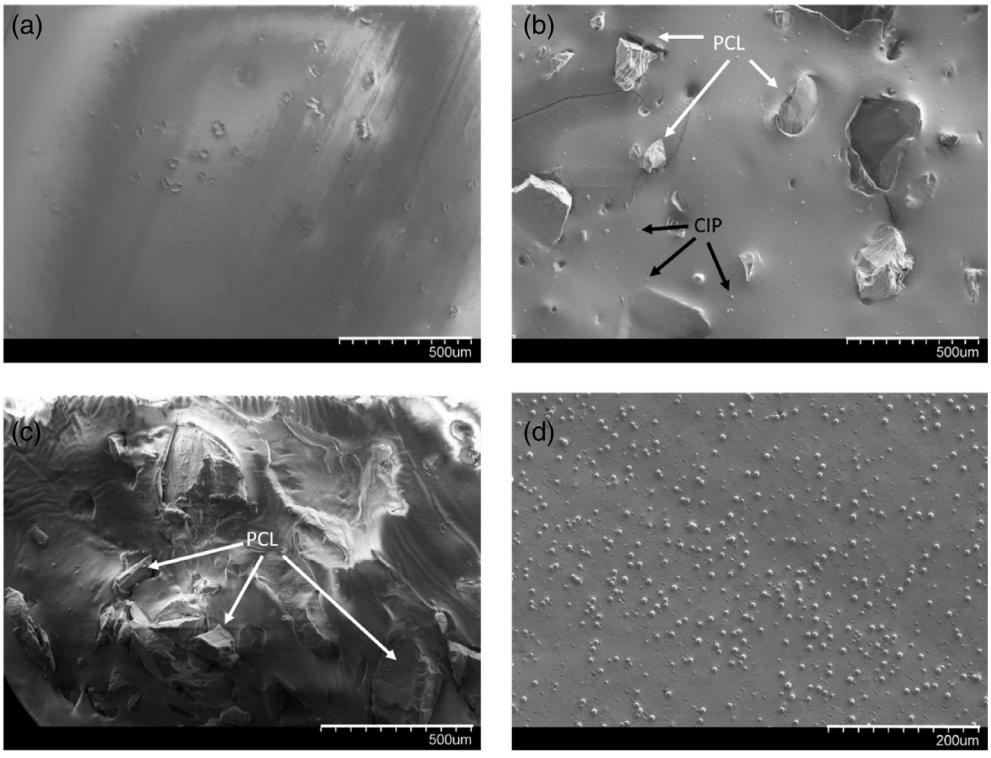

FIGURE 9 Scanning electron microscopy of (a) A (0), (b) PDMS with 10 wt% PCL and 10 wt% CIP, (c) E (20), and (d) PDMS with 20 wt% CIP. CIP, carbonyl iron particles; PCL, polycaprolactone; PDMS, polydimethylsiloxane

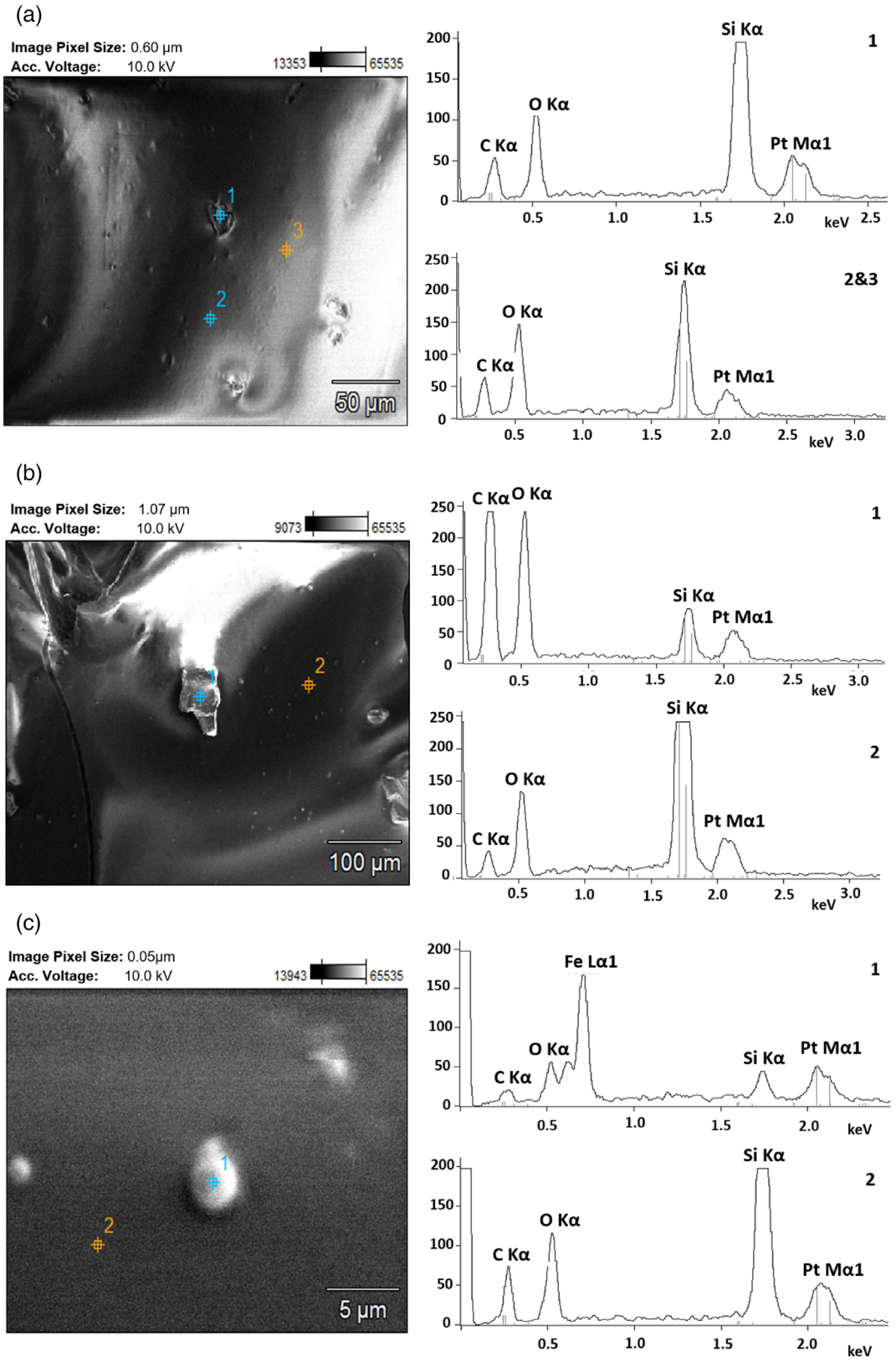

FIGURE 10 EDX of (a) pure PDMS, (b) PCL, and (c) CIP. CIP, carbonyl iron particles; EDX, energy-dispersive X-ray; PCL, polycaprolactone; PDMS, polydimethylsiloxane [Color figure can be viewed at wileyonlinelibrary.com]

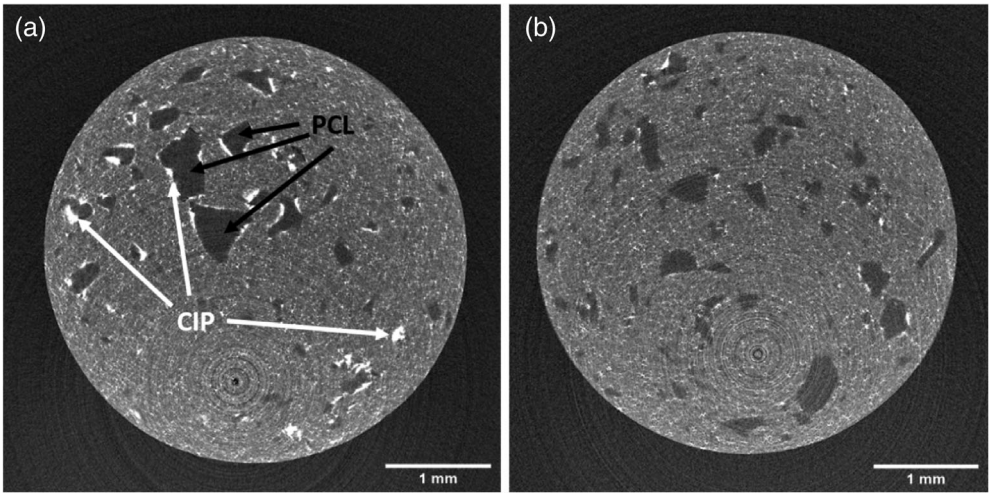

FIGURE 11 Reconstructed X-ray μ-CT images showing the center of each samples with (a) F (5, 15), (b) G (15, 5)

PCL and 10 wt% CIP particles, PDMS with 20 wt% CIP particles and the combination of 5 wt% PCL with 15 wt% CIP and 15 wt% PCL and 5 wt% CIP. The sample geometry is illustrated in Figure 1. These dimensions ensure a sufficiently large surface area to examine the sample for uniformity at several locations. The actual size of the measured samples is 1 x 4 x 2 mm^3, whereby only the surface is examined and therefore the height is not important. Several arbitrary sections with this dimension were extracted from the entire sample body and analyzed. The samples illustrated are untreated samples, that is, stored at room temperature, exclusively. The underlying reason is that the thermoplastic PCL particles melt and start to flow at a temperature of 58–60°C. Depending on the duration of the temperature treatment of 60°C, the PCL particles are not visible on the SEM images afterwards, because they have spread on the surface over time. Thus, the PCL particles cover the other components, which can no longer be detected or distinguished. Therefore, the images presented are merely micro morphological surface images of the different samples before the temperature treatment. In order to enable the samples to be analyzed by EDX and to avoid charging, the respective samples were sputtered with platinum. Since this platinum layer would appear as a peak in the EDX analysis, this peak was previously subtracted by the software, that is, each detected platinum peak is then caused by a different reason. The treatment with platinum makes the surfaces of the vacuum-resistant objects electrically conductive and allows them to be examined directly in the SEM. To prevent the samples from slipping, they are fixed to the holder with a special electrically conductive copper adhesive tape. The SEM images reveal a clear difference between the various sample compositions. While the PDMS can be perceived as a relatively smooth surface, which is illustrated in Figure 9(a), both the PCL and CIP are homogeneously distributed in the PDMS matrix. The surface of these compounds are very rough, see Figure 9(b)–(d). The charges on the PDMS sample with 20 wt% PCL, shown in Figure 9(c) were very high despite the necessary pretreatment, which is a significant difference to the other samples.

The PCL particles have an irregular shape with a size from about 120–600 μm were detected, whereas the CIP are uniform in shape and have a size of about 5 μm. On the evidence of the EDX images, see Figure 10, it can be proven that the smooth surface is exclusively pure PDMS, because the silicon (Si) peak is the highest, whereby the molecular formula of PDMS is $([CH_3]_2SiO)_n$. In addition, even platinum (Pt) can be detected, which may be an indication of the platinum catalyst of one component of the RTV-2 silicone, and both carbon (C) and oxygen (O) can be identified, which may also indicate components of the PDMS. If a PCL particle is detected, it increases the carbon and oxygen peak enormously. This can be clearly observed in Figure 10(b) and is confirmed by its molecular formula ($C_6H_{10}O_2$). If CIP are detected this is represented by the iron (Fe) peak in the EDX spectrum, which is shown in Figure 10(c).

2.6 | Micro computed tomography

Micro computed tomography (μ-CT) is proved to be a reliable method for analyzing the distribution of particles in this type of hybrid material. This method has enabled to tract the particles when they are subjected to varying external conditions like magnetic field[34,35] and mechanical strain. Hence, this method seems to be a promising approach to get a deeper understanding of the particles response to change in temperature. To investigate the influence of temperature on the distribution of thermoplastic particles, TomoTU setup was used to scan the samples. The reconstruction of a 3D model from

the radiographs was performed by a software package based on FDK algorithm.[36] The samples are cylindrical with a diameter of 4 mm and an height of 10 mm, see Figure 1. Figure 11 illustrates the reconstructed images of the scans made before melting the particles. The preliminary observation of the reconstructed images shows that, both the particles are distributed homogenously in the samples, which is also evident in the SEM images. In Figure 11(a), the PCL particles are represented as dark gray particles without specific shape and the bright regions show the agglomeration of CIPs surrounding the PCL particles. This is also evident in Figure 11(b). Agglomeration of CIPs could be a consequence of the preparation of the samples. During the preparation process, the respective powders are mixed with each other and then with the matrix. When the particles are mixed, electrostatic attraction forces can be created by the PCL particles, which then attach the much smaller CIP to it. The CIPs adhere to the PCL particles even after cross-linking of the matrix and form the agglomerates to be detected. The current work is progressing towards a detailed investigation on the influence of temperature on the distribution of PCL particles.

3 | CONCLUSION

The μ-CT and SEM examinations indicate that an homogeneous distribution of PCL and CIP within the thermosensitive elastomer prevails. The CIP agglomerates, that can be detected, are due to the manufacturing process and can therefore be generated or avoided. The hardness analysis and the shape memory tests confirm the fact that the TSE can be described as a SMP. The PCL particles resume their initial shape at room temperature after melting and cooling down to room temperature again, thereby the particles increase the hardness of the entire TSE both before and after the temperature treatment, while the CIP have only a minor influence here. The tensile and compression tests confirm the assumption that the TSE softens significantly during the melting process. It was determined that the mixture PDMS with 20 wt% PCL (sample E (20)) is the most suitable for this purpose, as the effect is the highest. The investigations of the heat transfer within the samples already indicate that a combination of TSE and MSE enables new applications. The process of heating the sample is accelerated by the addition of CIP in a TSE. But not only this property argues for a combination of thermoplastic and magnetic particles in an elastic matrix. The TSEs change their mechanical properties by the influence of a relatively low temperature of 60°C, similarly the MSEs change their mechanical properties by applying external magnetic fields.[28,29] For example, the stiffness of the TSE is reduced by increasing the temperature, while the stiffness of the MSE is increased by applying a magnetic field. The combination of both effects leads to bi-directional control. Future work will deal with the multistimulated compliance of such smart materials through the interaction of temperature and magnetic fields. The controlled manipulation of magnetic TSE's will enable their future use as grippers, actuators in the field of soft robotics.

ACKNOWLEDGMENT

The authors would like to express their thanks to the Deutsche Forschungsgemeinschaft (DFG) for financial support within the SP2100 research program (ZIM 540/20-1 and OD 18/28-1). A special word of thanks to Dr. Kerstin Pfeifer for the SEM and EDX analysis, to Dr. Jhohan Harvey Chavez Vega, Mr. Jiale Pan and Mr. Magnus Nauth for their contribution. Open Access funding enabled and organized by Projekt DEAL. [Corrections added on 25 June 2021, after first online publication: Projekt Deal statement been included.]

ORCID

Nina Prem https://orcid.org/0000-0001-9438-9536

REFERENCES

[1] K. Zimmermann, V. Bohm, I. Zeidis, Vibration-driven mobile robots based on magneto-sensitive elastomers. Paper presented at: 2011 IEEE/ASME International Conference on Advanced Intelligent Mechatronics (AIM 2011), *Budapest, Hungary*, 3–7 July 2011; IEEE: Piscataway, NJ, **2011**, pp 730–735.

[2] I. A. Brigadnov, A. Dorfmann, *Int. J. Solids Struct.* **2003**, *40*, 4659.

[3] T. I. Becker, V. Böhm, J. Chavez Vega, S. Odenbach, Y. L. Raikher, K. Zimmermann, *Arch. Appl. Mech.* **2019**, *89*, 133.

[4] C. Bellan, G. Bossis, *Int. J. Mod. Phys.* **2002**, *2012*, 2447.

[5] D. Ivaneyko, V. P. Toshchevikov, M. Saphiannikova, G. Heinrich, *Magneto-sensitive Elastomers in a Homogeneous Magnetic Field: A Regular Rectangular Lattice Model, Macromolecular Theory and Simulations*, **2011**. https://doi.org/10.1002/mats.201100018.

[6] N. Prem, J. C. Vega, V. Böhm, D. Sindersberger, G. J. Monkman, K. Zimmermann, *Macromol. Chem. Phys.* **2018**, *219*, 1800222.

[7] T. Hu, S. Xuan, L. Ding, X. Gong, *Mater. Des.* **2018**, *156*, 528.

[8] N. Prem, D. Sindersberger, G. J. Monkman, *Adv. Mater. Sci. Eng.* **2019**, *2019*, 1.

[9] P. Zarrintaj, M. Jouyandeh, M. R. Ganjali, B. S. Hadavand, M. Mozafari, S. S. Sheiko, M. Vatankhah-Varnoosfaderani, T. J. Gutiérrez, M. R. Saeb, *Eur. Polym. J.* **2019**, *117*, 402.

[10] Z. Zhang Ed., *Switchable and responsive surfaces and materials for biomedical applications*, Elsevier, Amsterdam, Boston, Cambridge, Heidelberg, London, New York, Oxford, Paris, San Diego, San Francisco, Singapore, Tokyo **2015**.

[11] T. Bayerl, *Application of particulate susceptors for the inductive heating of temperature sensitive polymer-polymer composites*, Zugl.: Kaiserslautern, Techn. Univ., Diss., 2012; Univ. Inst. für Verbundwerkstoffe, Kaiserslautern **2012**.
[12] J. Ackermann, V. Damrath, *Chem. Unserer Zeit* **1989**, *23*, 86.
[13] Wacker. Raumtemperaturvernetzende Siliconkautschuke (RTV-1/RTV-2), **2020**. https://www.wacker.com/cms/de-de/products/product-groups/silicone-rubber/room-temperature-silicone-rubber.html (accessed: October 21, 2020.741Z).
[14] X. Poulain, V. Lefèvre, O. Lopez-Pamies, K. Ravi-Chandar, *Int. J. Fract.* **2017**, *205*, 1.
[15] B. Wang, H. Lu, G.-H. Kim, *Mech. Mater.* **2002**, *34*, 475.
[16] M. Klüppel, *Macromol. Symp.* **2003**, *194*, 39.
[17] W. F. Reichert, D. Göritz, E. J. Duschl, *Polymer* **1993**, *34*, 1216.
[18] D. Erickson, D. Sinton, D. Li, *Lab Chip* **2003**, *3*, 141.
[19] P. Yi, R. A. Awang, W. S. T. Rowe, K. Kalantar-zadeh, K. Khoshmanesh, *Lab Chip* **2014**, *14*, 3419.
[20] P. Douglas, A. B. Albadarin, A. A. H. Al-Muhtaseb, C. Mangwandi, G. M. Walker, *J. Mech. Behav. Biomed. Mater.* **2015**, *45*, 154.
[21] M. D. Bartlett, N. Kazem, M. J. Powell-Palm, X. Huang, W. Sun, J. A. Malen, C. Majidi, *Proc. Natl. Acad. Sci. U. S. A.* **2017**, *114*, 2143.
[22] Q. Mu, S. Feng, G. Diao, *Polym. Compos.* **2007**, *28*, 125.
[23] H. Zhong, P. Yu, Z. Hu, P. Zhang, Z. Yang, *Smart Mater. Struct.* **2018**, *28*.
[24] J. Diani, B. Fayolle, P. Gilormini, *Eur. Polym. J.* **2009**, *45*, 601.
[25] T. Lu, J. Wang, R. Yang, T. J. Wang, *J. Appl. Mech.* **2017**, *84*.
[26] T.-T. Mai, Y. Morishita, K. Urayama, *Soft Matter* **2017**, *13*, 1966.
[27] G. Marckmann, E. Verron, L. Gornet, G. Chagnon, P. Charrier, P. Fort, *J. Mech. Phys. Solids* **2002**, *50*, 2011.
[28] J. M. Ginder, M. E. Nichols, L. D. Elie, S. M. Clark, in *Smart Structures and Materials 2000: Smart Structures and Integrated Systems* (Ed: N. M. Wereley), SPIE, Newport Beach, CA, United States **2000**, p. 418.
[29] J. Winger, M. Schümann, A. Kupka, S. Odenbach, *J. Magn. Magn. Mater.* **2019**, *481*, 176.
[30] T. Ohki, Q.-Q. Ni, N. Ohsako, M. Iwamoto, *Composites, Part A* **2004**, *35*, 1065.
[31] T. Xie, *Nature* **2010**, *464*, 267.
[32] J. Ruge, H. Wohlfahrt, *Technologie der Werkstoffe*, Springer Fachmedien Wiesbaden, Wiesbaden **2013**.
[33] A. Siddiqui, M. Braden, M. P. Patel, S. Parker, *Dent. Mater.* **2010**, *26*, 560.
[34] D. Borin, D. Günther, C. Hintze, G. Heinrich, S. Odenbach, *J. Magn. Magn. Mater.* **2012**, *324*, 3452.
[35] T. Gundermann, S. Odenbach, *Smart Mater. Struct.* **2014**, *23*, 105013.
[36] L. A. Feldkamp, L. C. Davis, J. W. Kress, *J. Opt. Soc. Am. A* **1984**, *1*, 612.

How to cite this article: N. Prem, F. Schale, K. Zimmermann, D. K. Gowda, S. Odenbach, *J Appl Polym Sci* **2021**, *138*(44), e51296. https://doi.org/10.1002/app.51296